

Synthesis of silicon nanowires supported Ag nanoparticles and their catalytic activity in photo-degradation of Rhodamine B

Yueyin SHAO (✉)¹, Yongqian WEI¹, Zhenghua WANG²

¹ Laboratory Material Supply Centre, Soochow University, Suzhou 215123, China

² Anhui Key Laboratory of Functional Molecular Solids, College of Chemistry and Materials Science, Anhui Normal University, Wuhu 241000, China

© Higher Education Press and Springer-Verlag Berlin Heidelberg 2011

Abstract Silver modified silicon nanowires were obtained and employed as photo-catalysts in the degradation of Rhodamine B (RhB), which demonstrated the excellent catalytic activity. These catalysts may be recycled and reused.

Keywords silicon nanowires, Ag nanoparticles, Rhodamine B (RhB)

1 Introduction

Noble metal nanoparticles have attracted increasing interest due to their size and shape dependent optical and electronic properties, which are expected to have wide applications in optics, microelectronics, sensors, and catalysis [1,2]. In recent years, nanometer-scale silver particles have attracted the interest of researchers because of their unique properties: large surface-to-volume ratio, high surface reaction activity, high catalytic efficiency and strong adsorption ability. Therefore, they have potential applications in many areas, such as: nonlinear optical switching [3], immunoassay labeling [4], second harmonic generation [5] and a wealth of optical phenomena directly related to their geometry-dependent surface plasmon resonance.

Synthesis of noble metal nanoparticles has been the subject of many scientific reports in consideration for applications. Several preparation methods have been devised for silver nanoparticles, including surfactant-based seed mediated growth [6–8], thermal methods [9], and photoreduction processes [10]. The assembly of noble

metal nanoparticles on planar surfaces was the key step in their application. And it still requires more sophisticated methods, such as lithography [11,12], electroless deposition [13], electroplating on insulators and the formation of colloids under constant reagent flow [14].

In spite of the above effects, yet, the agglomeration of nanoparticles during the preparation remains a formidable problem [15]. Over the past years, an alternative method for generating stabilized metal nanoparticles involves synthesis in nanoporous supports, which help define particle size and serve to immobilize the resulted particles.

Herein, we present a new strategy for synthesizing Ag nanoparticles with easy recycle by using silicon nanowires (SiNWs) as a carrier. As a kind of typical one-dimensional nanomaterials, SiNWs were produced via numerous methods [16–18], which provided a number of remarkable advantages, such as easy surface modification with various metal particles [19], a vast surface-volume ratio [20], and stability to atmosphere environment. In this work, SiNWs were successfully prepared and then modified with Ag nanoparticles. This new surface was a significant improvement over traditional unsupported Ag nanoparticles for applications. The experiments showed that this Ag/Si nanostructure exhibited highly active catalysis and excellent stability recycle in the degradation of Rhodamine B (RhB). This meant that the substrate has much effect on the behavior of Ag nanoparticles.

2 Experiment

2.1 Synthesis of Ag nanoparticles

0.005 g as-synthesized SiNWs, obtained via the high-temperature method, were etched with 10 mL 5% HF aqueous solution for 30 min, then rinsed with de-ionized

water and immersed in 10 mL 10^{-3} mol/L AgNO_3 aqueous solution. When the yellow SiNWs gradually turned black, they were modified with Ag nanoparticles. Unsupported Ag nanoparticles were prepared by reducing silver nitrate 0.25 mL (1×10^{-3} mol/L) with sodium borohydride 0.15 mL (1×10^{-2} mol/L). The solutions were mixed with continuous stirring until the solution turned yellow at room temperature [21].

2.2 Degradation process

In a representative degradation experiment, 3.0 mL 10^{-6} mol/L RhB was added into a quartz cuvette with an optical path of 1 cm long, and then the as-prepared Ag/Si catalysts were added. The progress of the degradation was monitored using a fluorescence and UV-vis spectrophotometer.

2.3 Characterization

The phase and crystallography of the products were characterized by a Shimadzu XRD-6000 X-ray diffractometer equipped with Cu K α radiation ($\lambda = 0.15406$ nm). A scanning rate of $0.05^\circ \cdot \text{s}^{-1}$ was applied to record the pattern in the 2θ range of 20° – 100° . The morphologies of as-prepared products were analyzed with an S-4800 field emitting scanning electron microscopy (FESEM), equipped with an energy dispersive X-ray (EDX) spectroscope. Transmission electron microscopy (TEM), selected area electron diffraction (SAED) pattern and high-resolution transmission electron microscope (HRTEM) image were captured with a JEOL-2010 transmission electron microscope with an accelerating voltage of 200 kV. Degradation process was tracked with a U-4100 spectrophotometer. The PL spectra of the sample were recorded using a Hitachi F-4500 fluorescence spectrophotometer at room temperature.

3 Results and discussion

3.1 Synthesis of Ag nanoparticles

Figure 1(a) shows the X-ray diffraction (XRD) pattern of the as-prepared SiNWs, and all the diffraction peaks can be indexed as the cubic phase of Si. The cell parameter is calculated to be $a = 0.5415 \pm 0.0009$ nm, which is in agreement with the value of face-centered cubic silicon $a = 0.5430$ nm (JCPDS card No. 27-1402). Figure 1(b) shows the XRD pattern of the SiNW-supported Ag nanoparticles. No other characteristic peaks were observed except for Si and Ag, which indicates that the product has a high degree of crystallinity. The calculated lattice constant of Ag is $a = 0.4080 \pm 0.0004$ nm, which is consistent with the reported value, $a = 0.4086$ nm (JCPDS card No. 04-0783).

Figure 2 is the SEM image of silicon nanostructure, which exhibits their wire-like morphology. The average

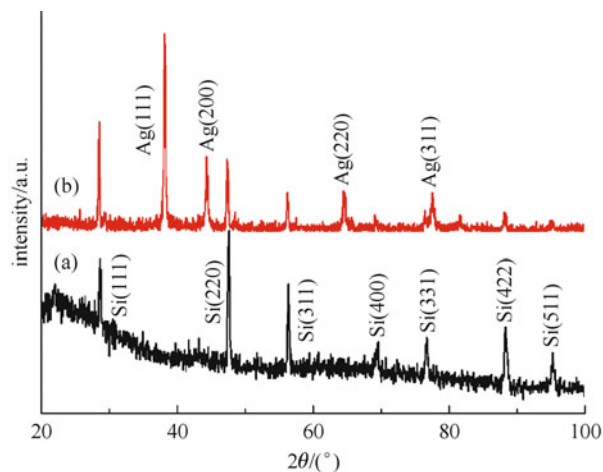


Fig. 1 XRD patterns of (a) SiNWs and (b) Ag/Si nanostructure

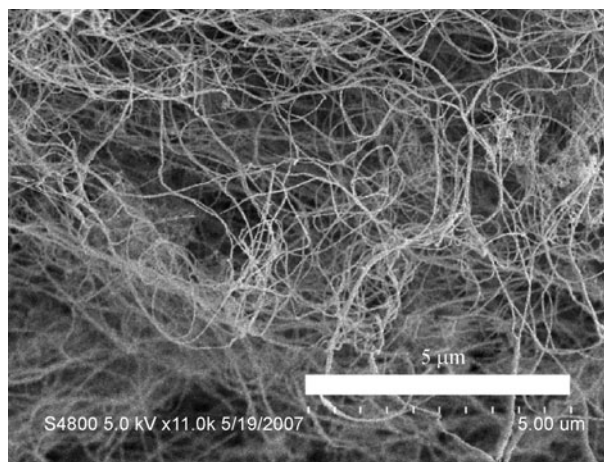


Fig. 2 SEM image of SiNWs

diameter of SiNWs is 50 nm.

Figure 3 presents a TEM image of one single wire with the average diameter of 86 nm modified with Ag nanoparticles, which are randomly attached to the surface of SiNW, taking an average diameter of 50 nm. Figure 3(a) shows the TEM image of single SiNW supported with Ag nanoparticles. The EDX (Fig. 3(b)) was further used to check the chemical composition of the products. The detected oxygen comes from the adsorption of the sample when exposed to the air. No peaks of other elements are detected except for Si and Ag. A close examination of the sample using HRTEM (Fig. 3(c)) reveals the lattice fringe of Si and Ag, both showing (111) crystal planes. The selected area electron diffraction (SAED) (Fig. 3(d)) taken from this area displays the crystalline structure of Si and Ag. The bright spots can be indexed as (1–11) and (111) of silicon respectively, taking the zone axis of (110), while the diffraction ring is consistent with the (200) plane of Ag nanoparticles.

All of the above characterization results are consistent

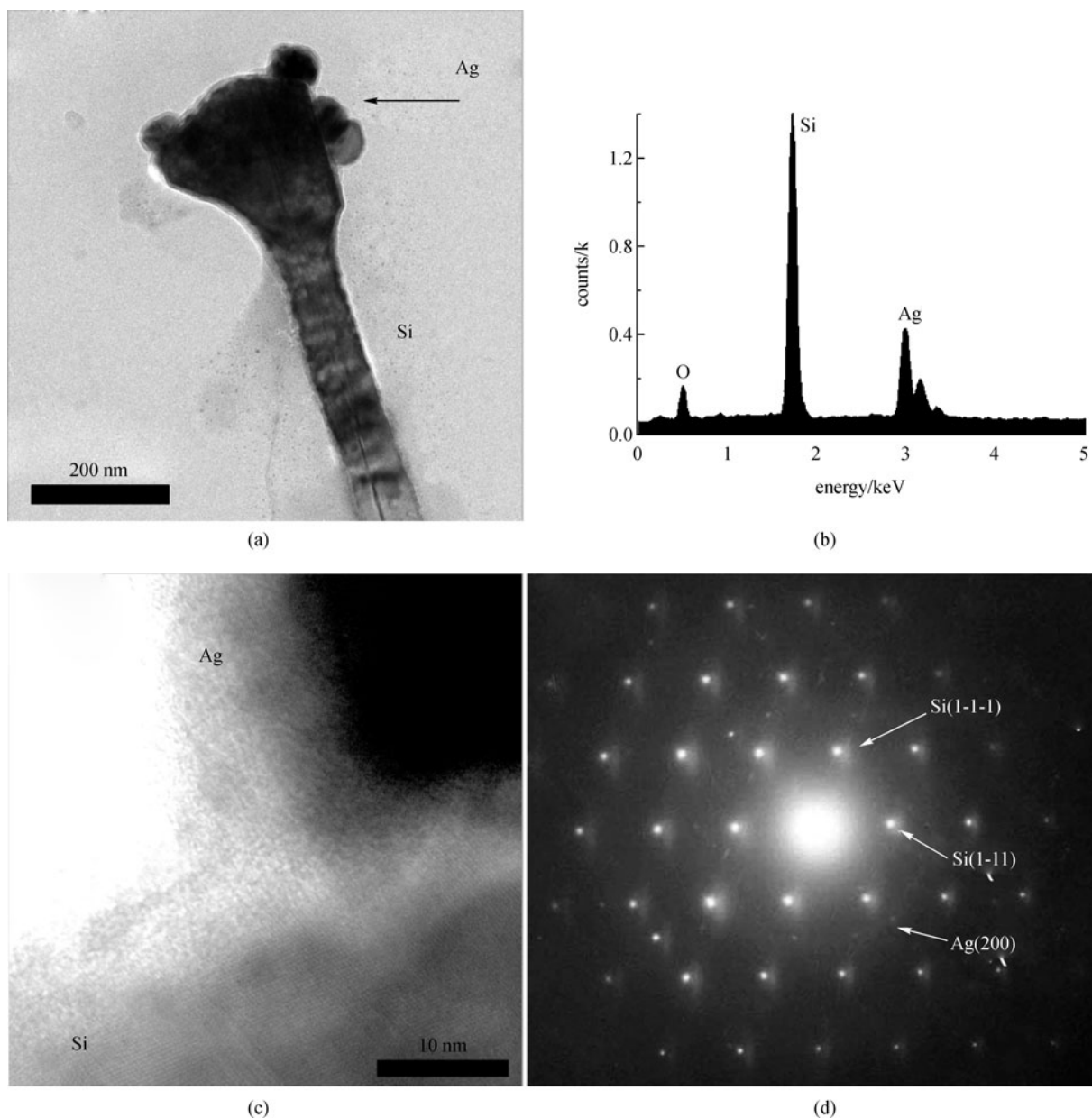


Fig. 3 (a) TEM image of single SiNW supported with Ag nanoparticles; (b) EDX of SiNW revealing its chemical composition of Si and Ag; (c) HRTEM image showing both (111) crystal planes of Si and Ag; (d) SAED pattern indicating bright diffraction spots of Si and weak diffraction ring of Ag nanoparticles

with each other and adequately prove the fact that the SiNWs have been modified with Ag nanoparticles.

3.2 Degradation of Rhodamine with Ag/Si nanostructure

To demonstrate the potential applicability of the present Ag/Si nanoparticles, we investigated the application of degrading RhB. The characteristic absorption of RhB at $\lambda = 551$ nm was chosen to monitor the degradation process. Figure 4(a) shows the successive UV-visible spectra of an aqueous solution of RhB. The absorption peak at $\lambda = 553$ nm diminishes gradually as the time gets prolonged,

and completely disappears at about 20 min, which indicates the complete degradation of RhB during the reaction. Figure 4(b) shows that the relationship of $\ln(C_{\text{RhB}})$ versus reaction time is nearly linear, and the slope is -0.23673 ± 0.01022 ; the intercept is -1.40436 ± 0.1209 . So the reduction rate of RhB may be expressed as $r = 0.0581 \exp(-0.23673\tau)$.

In order to have a comparison, a contrast experiment was performed. We kept other conditions constant and replaced Ag/Si nanoparticles with Ag-nanoparticles. Figure 5 shows that the reaction does not take place. The result adequately proves the activity of the as-prepared nanoparticles.

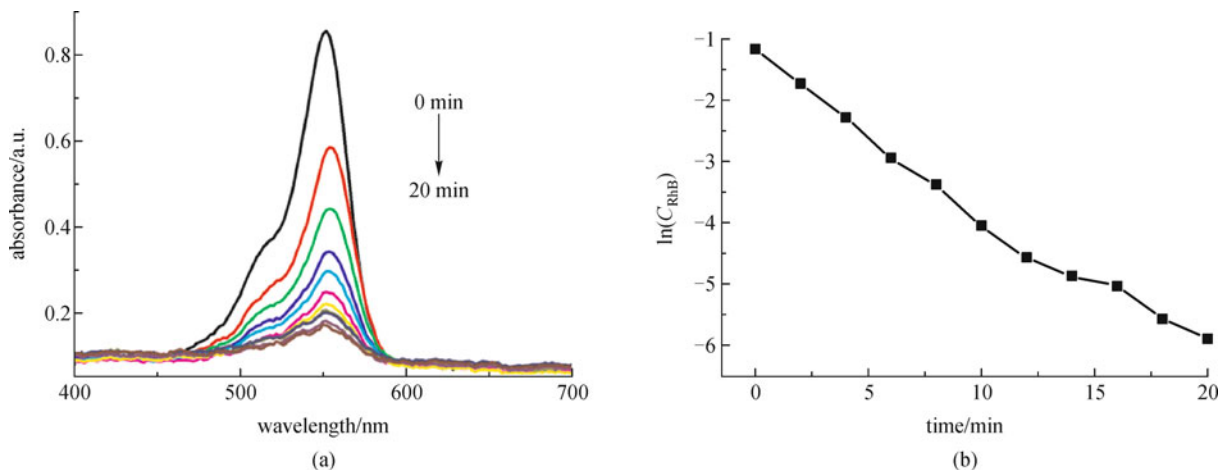


Fig. 4 (a) UV-vis spectra of degradation of RhB using Ag/Si catalysts at room temperature; (b) curve of $\ln(C_{\text{RhB}})$ concentration versus time using Ag/Si catalysts

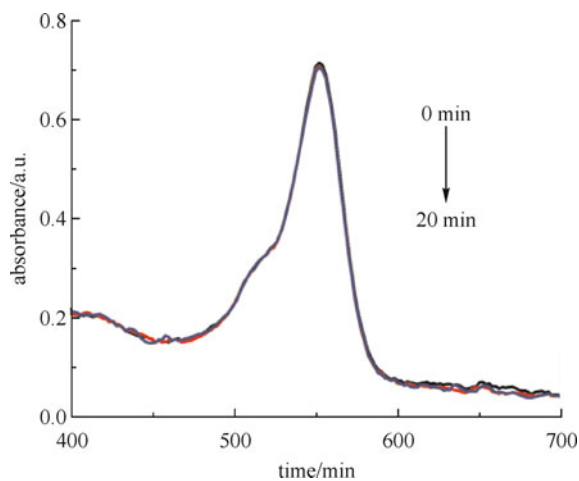


Fig. 5 UV-vis spectra of degradation of RhB using nano-Ag catalysts at room temperature

Since the Ag nanoparticles were supported on the SiNWs, the catalysts can be easily recycled and initiate the next degradation after being rinsed with distilled water. The reaction was studied using recycled catalysts. Along with the increment of the recycle times, the activity of the as-prepared samples diminishes slowly (Fig. 6(a)). The relationship of the reaction constant versus cycle times is shown in Fig. 6(b), which may be expressed as $k = 0.2578 - 0.0248N$, where k is the reaction rate constant and N is the cyclic time.

The above results obviously indicate that the catalytic activity and stability of Ag/Si catalysts are promising, which may find wider application in the catalytic field.

Although the precise mechanism for the degradation of RhB is still under discussion, the direct catalysis of Ag/Si is assuredly crucial. Ag nanoparticles in our experiment, with an average diameter of 50 nm, have a large surface-to-volume ratio compared to bulk metal. The SiNWs supported Ag nanoparticles are kept from congregating

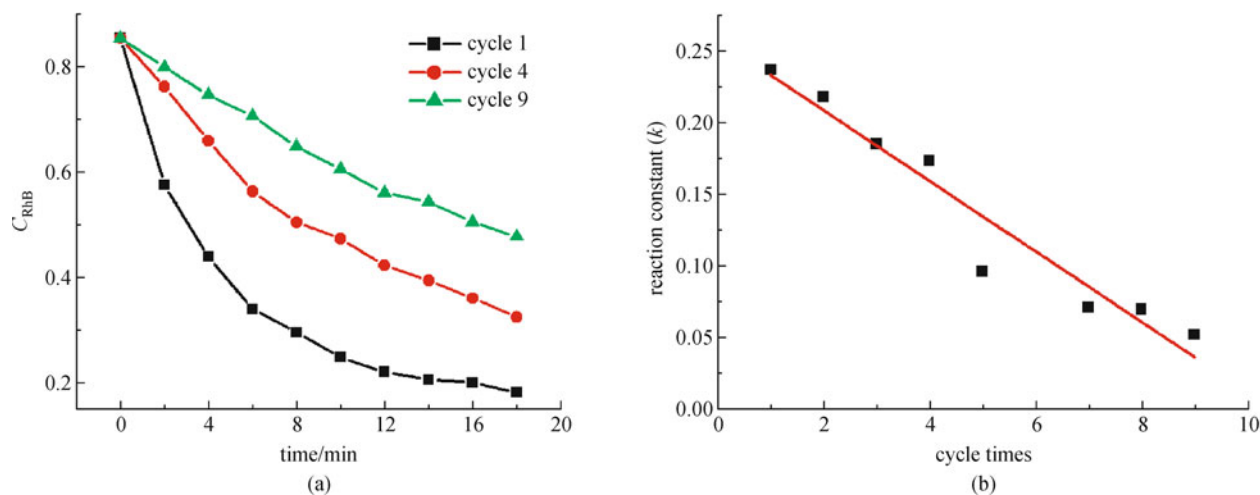


Fig. 6 (a) Recycling experiments of Ag/Si catalysts in degradation of RhB; (b) curve of reaction constant versus cycle times

and growing large because they are fixed on the SiNWs, which may facilitate Ag catalysts with a high efficiency during the reaction and in the use of recycling.

4 Conclusions

Ag/Si nanostructure was prepared using SiNWs as a carrier, which had reasonably high surface area and small crystal size. It made SiNWs an attractive host in support of nanoparticles. The results indicated that these SiNWs supported Ag catalysts provided strong activity in the process of degradation of RhB, which showed high mobility and excellent recycling stability. Moreover, the maneuverability and controllability of this fabrication enables Ag/Si catalysts to find applications in other fields.

Acknowledgements This work was supported by the National Natural Science Foundation of China (Grant No. 20701001).

References

1. Rondinini S, Vertova A. Electrocatalysis on silver and silver alloys for dichloromethane and trichloromethane dehalogenation. *Electrochimica Acta*, 2004, 49(22–23): 4035–4046
2. Adhyapak P V, Karandikar P, Vijayamohan K, Athawale A A, Chandwadkar A J. Synthesis of silver nanowires inside mesoporous MCM-41 host. *Materials Letters*, 2004, 58(7–8): 1168–1171
3. Carotenuto G, Pepe G P, Nicolais L. Preparation and characterization of nano-sized Ag/PVP composites for optical applications. *European Physical Journal B*, 2000, 16(1): 11–17
4. Grubisha D S, Lipert R J, Park H Y, Driskell J, Porter M D. Femtomolar detection of prostate-specific antigen: an immunoassay based on surface-enhanced Raman scattering and immunogold labels. *Analytical Chemistry*, 2003, 75(21): 5936–5943
5. García-Vidal F J, Pendry J B. Collective theory for surface enhanced Raman scattering. *Physical Review Letters*, 1996, 77(6): 1163–1166
6. Jana N R, Gearheart L, Murphy C J. Seed-mediated growth approach for shape-controlled synthesis of spheroidal and rod-like gold nanoparticles using a surfactant template. *Advanced Materials*, 2001, 13(18): 1389–1393
7. Jana N R, Gearheart L, Murphy C J. Evidence for seed-mediated nucleation in the chemical reduction of gold salts to gold nanoparticles. *Chemistry of Materials*, 2001, 13(7): 2313–2322
8. Murphy C J, Jana N R. Controlling the aspect ratio of inorganic nanorods and nanowires. *Advanced Materials*, 2002, 14(1): 80–82
9. Jin R C, Cao Y C, Hao E C, Métraux G S, Schatz G C, Mirkin C A. Controlling anisotropic nanoparticle growth through plasmon excitation. *Nature*, 2003, 425(6957): 487–490
10. Maillard M, Huang P R, Brus L. Silver nanodisk growth by surface plasmon enhanced photoreduction of adsorbed. *Nano Letters*, 2003, 3(11): 1611–1615
11. Hua F, Cui T H, Lvov Y. Lithographic approach to pattern self-assembled nanoparticle multilayers. *Langmuir*, 2002, 18(17): 6712–6715
12. Haynes C L, Van Duyne R P. Dichroic optical properties of extended nanostructures fabricated using angle-resolved nanosphere lithography. *Nano Letters*, 2003, 3(7): 939–943
13. Porter L A, Choi H C, Ribbe A E, Buriak J M. Controlled electroless deposition of noble metal nanoparticle films on germanium surfaces. *Nano Letters*, 2002, 2(10): 1067–1071
14. Keir R, Igata E, Arundell M, Smith W E, Graham D, McHugh C, Cooper J M. SERRS. *In situ* substrate formation and improved detection using microfluidics. *Analytical Chemistry*, 2002, 74(7): 1503–1508
15. Zhu G S, Wang C, Zhang Y H, Guo N, Zhao Y Y, Wang R W, Qiu S L, Wei Y, Baughman R H. Highly effective sulfated zirconia nanocatalysts grown out of colloidal silica at high temperature. *Chemistry*, 2004, 10(19): 4750–4754
16. Liu Z Q, Zhou W Y, Sun L F, Tang D S, Zou X P, Li Y B, Wang C Y, Wang G, Xie S S. Growth of amorphous silicon nanowires. *Chemical Physics Letters*, 2001, 341(5–6): 523–528
17. Kamins T I, Williams R S, Chen Y, Chang Y L, Chang Y A. Chemical vapor deposition of Si nanowires nucleated by TiSi₂ islands on Si. *Applied Physics Letters*, 2000, 76(5): 562–564
18. Shao M W, Hu H, Li M, Ban H Z, Wang M Y, Jiang J. Karman vortex street assisted patterning in the growth of silicon nanowires. *Chemical Communications*, 2007, (8): 793–794
19. Li C P, Sun X H, Wong N B, Lee C S, Lee S T, Teo B K. Silicon nanowires wrapped with Au film. *Journal of Physical Chemistry B*, 2002, 106(28): 6980–6984
20. Cui Y, Wei Q Q, Park H K, Lieber C M. Nanowire nanosensors for highly sensitive and selective detection of biological and chemical species. *Science*, 2001, 293(5533): 1289–1292
21. Ren X, Meng X W, Chen D, Tang F Q, Jiao J. Using silver nanoparticle to enhance current response of biosensor. *Biosensors & Bioelectronics*, 2005, 21(3): 433–437